RESEARCH ARTICLE | MAY 20 2022

An energy-conservative many-body dissipative particle dynamics model for thermocapillary drop motion

Kaixuan Zhang (张凯旋) ; Jie Li (李杰); Wei Fang (方维); Chensen Lin (林晨森) ; Jiayi Zhao (赵嘉毅) ; Zhen Li (李振) ; Yang Liu (刘扬); Shuo Chen (陈硕) ; Cunjing Lv (吕存景) ; Xi-Qiao Feng (冯西桥)

Physics of Fluids 34, 052011 (2022)
https://doi.org/10.1063/5.0088238

Physics of Fluids ARTICLE scitation.org/journal/phf

An energy-conservative many-body dissipative particle dynamics model for thermocapillary drop motion

Cite as: Phys. Fluids **34**, 052011 (2022); doi: 10.1063/5.0088238
Submitted: 14 February 2022 · Accepted: 19 April 2022 ·
Published Online: 20 May 2022

View Online Export Citation CrossMark

Kaixuan Zhang (张凯旋),[1,2] Jie Li (李杰),[1] Wei Fang (方维),[2] Chensen Lin (林晨森),[1,3,a)] Jiayi Zhao (赵嘉毅),[4] Zhen Li (李振),[5] Yang Liu (刘扬),[6] Shuo Chen (陈硕),[1,3,a)] Cunjing Lv (吕存景),[2] and Xi-Qiao Feng (冯西桥)[2]

AFFILIATIONS

[1]School of Aerospace Engineering and Applied Mechanics, Tongji University, Shanghai 200092, China
[2]Institute of Biomechanics and Medical Engineering, AML, Department of Engineering Mechanics, Tsinghua University, Beijing 100084, China
[3]Shanghai Key Lab of Vehicle Aerodynamics and Vehicle Thermal Management Systems, Tongji University, Shanghai 201804, China
[4]School of Energy and Power Engineering, University of Shanghai for Science and Technology, Shanghai 200093, China
[5]Department of Mechanical Engineering, Clemson University, Clemson, South Carolina 29634, USA
[6]Department of Mechanical Engineering, The Hong Kong Polytechnic University, Hong Kong, China

[a)]**Authors to whom correspondence should be addressed:** linchensen@outlook.com and schen_tju@mail.tongji.edu.cn

ABSTRACT

The thermocapillary motion of a drop on a solid substrate is a common phenomenon in daily life and many industrial fields. The motion can be significantly affected by the temperature gradient of the substrate and the properties of the liquid, such as surface tension, viscosity, thermal coefficient, density, and diffusivity. In this study, a numerical model based on modified many-body dissipative particle dynamics was developed to capture correctly the temperature dependence of a fluid. The momentum, thermal diffusivity, viscosity, and surface tension of liquid water at various temperatures ranging from 273 to 373 K were used as examples to verify the proposed model. The results calculated with this model for heat conduction in a liquid–solid system are in good agreement with those calculated with Fourier's law. The approach successfully modeled the thermocapillary motion of a liquid water droplet on a hydrophobic substrate with a temperature gradient. The migration of the droplet on a flat solid substrate was induced by the difference in surface tension due to the temperature gradient. The migration velocity increased with the temperature difference, which is in agreement with the present theoretical analysis and dynamic van der Waals theory. The modified numerical model proposed in this work could be used to study heat and mass transfer across a free interface, such as Marangoni convection in multiphase fluid flow.

I. INTRODUCTION

Dissipative particle dynamics (DPD) proposed by Hoogerbrugge and Koelman[1] is a particle-based method for micro- and nano-fluid simulations. By combining the advantages of a large timescale in lattice-gas automata and the mesh-free property in molecular dynamics, DPD is more efficient for simulating larger fluid systems than molecular dynamics. As a coarse-grained model, every DPD particle represents a cluster of atoms or molecules and thereby the computation effort is greatly reduced. Due to the larger spatial and temporal scales, DPD is a flexible method for investigating simple fluids[2] and complex fluids, such as polymer[3,4] and DNA suspensions,[5] the dynamics of red blood cells,[6–11] and biofluids.[12]

In DPD, the interactions between particles determine the basic properties of the fluid system. These include a conservative force, a dissipative force, and a random force. The conservative force is a soft repulsive force that makes a contribution to the fluid compressibility. The dissipative force generates friction between DPD particles, which can represent the viscosity of the system. The random force makes up for the deficiencies of the coarse-grained treatment by introducing a stochastic force on each DPD particle. The latter two forces satisfy the fluctuation–dissipation theorem and act as a thermostat to keep the system at a constant temperature.[13] Since there is no attractive force between DPD particles, the equation of state in classic DPD does not match the van der Waals curve and cannot simulate a system where

liquid and vapor coexist. By introducing an attractive force term and adding the local density into the repulsive term, the modified conservative force produces a *many-body* interaction with *long-range* attraction and *short-range* repulsion.[14] The pressure of the system has a cubic relation with density and can generate a free interface. This many-body dissipative particle dynamics (mDPD) method has been widely used to simulate droplet dynamics on substrates,[15–18] pinch-off dynamics,[19] bubble collapse,[20] and multiphase flow in a complex geometry.[21,22]

Both classic DPD and its *many-body* version, i.e., mDPD, can describe only isothermal systems due to the thermostat in the models. To simulate heat transfer, an extra temperature quantity is introduced for each DPD particle. This results in energy-conserved dissipative particle dynamics (eDPD),[23] which has been adopted to investigate heat conduction,[24–27] natural convection,[28–32] and solidification.[33] Ripoll *et al.*[34] confirmed with a 1D simulation that heat conduction in eDPD obeys Fourier's law. He and Qiao[35] adopted eDPD to investigate heat conduction between a nano-fluid and nano-materials. Abu-Nada[28] considered Neumann and Dirichlet boundary conditions and simulated 2D heat conduction using eDPD. They also modified the parameters in eDPD to study natural convection and then validated their results by comparing them with computational fluid dynamics simulations. Li *et al.*[36] proposed analytical formula for determining the mesoscopic heat friction and validated their prediction by reproducing the experimental data for the Prandtl number of liquid water at various temperatures. Johansson *et al.*[33] adopted eDPD to simulate phase transfers. The solidification process they captured agrees with a theoretical analysis. They also suggested that a modified model is needed to reproduce the release of the latent heat during the transition from the liquid to the solid phase. These systems with heat transfer do not have a free interface, which can be simulated by eDPD. However, for multiphase systems, such as a liquid droplet wetting on a hot substrate, it is still a challenge for eDPD or mDPD to capture heat transfer.

To simulate heat transport in non-isothermal multiphase fluid systems, energy-conserving many-body dissipative particle dynamics (mDPDe) was developed by combining eDPD with mDPD. Yamada *et al.*[37] simulated heat conduction between droplets and a solid substrate using mDPDe. The droplet density at different temperatures seemed to be constant in their simulations, which does not match that of most liquids in the real world. Wang *et al.*[38,39] adopted mDPDe to investigate ice crystal nucleation leading to droplets freezing on flat substrates. Their results for the nucleation and shape deformation of a water droplet during freezing agreed well with the experimental data. Their work illustrated that modified mDPDe can be used to study the freezing of a water droplet. However, the corresponding temperature-dependent properties of the system were not accurately determined by the numerical model although these are important for assessing the validity of the model.

The objective of the present work is to propose a modified mDPDe model that can correctly capture the temperature-dependent properties of a fluid system with a free interface, such as the Marangoni effect for a droplet. Specifically, liquid water is used as an example for verifying the mDPDe model we propose. The density, surface tension, diffusivity, and viscosity of liquid water as well as the Schmidt and Prandtl numbers in the range 273 to 373 K were determined by the mDPDe model. The relation between surface tension and the conservative force was analyzed. The temperature-dependent density and surface tension were obtained, as these can be important for investigating fluids with complex mass transfer. The relation of the weight function with temperature proposed by Li *et al.* is adopted.[36] Results for the diffusivity and viscosity as well as the Schmidt number at various temperatures are presented and compared with the experimental data available for liquid water. Furthermore, a fitting formula for correcting the mesoscopic heat friction was obtained. It reproduces more accurately the Prandtl number of liquid water at various temperatures. This proposed model is not limited to liquid water and can readily be extended to model the thermal hydrodynamic properties in various situations including heat and mass transfer dynamics.[40–44]

The paper is organized as follows. In Sec. II, we describe the mDPDe formulation and parameters, including analytical formulas for determining the surface tension and the mesoscopic heat friction. Section III presents our validation of the mDPDe model, and its performance in reproducing the temperature-dependent properties found experimentally. Furthermore, we simulate the thermocapillary motion of a droplet on a hydrophobic substrate with temperature gradients, and we compare the results for the velocity with those from a theoretical analysis and simulations based on dynamic van der Waals theory (DVDWT). Finally, we conclude with a brief summary in Sec. IV.

II. BASIC GOVERNING EQUATIONS OF THE METHOD

In the mDPDe method, each particle interacts with others through distance- and velocity-dependent forces within a certain cutoff of distance.[1,23,45] The momentum and energy transfers between mDPDe particles obey momentum and energy conservation, respectively. The evolution of a particle's motion is governed by Newton's second law

$$m_i \frac{\mathrm{d}\vec{v}_i}{\mathrm{d}t} = \sum_{j\neq i}\left(\vec{f}_{ij}^{\,C} + \vec{f}_{ij}^{\,D} + \vec{f}_{ij}^{\,R}\right) + \vec{f}_{ext}, \tag{1}$$

where $m_i = 1$ and $\vec{f}_{ext}$ is an external force and $\vec{f}_{ij}^{\,C}$, $\vec{f}_{ij}^{\,D}$, and $\vec{f}_{ij}^{\,R}$ are the conservative, dissipative, and random forces between particle i and j, respectively. Their specific expressions can be written as follows:

$$\vec{f}_{ij}^{\,C} = A_{ij}\omega^C(r_{ij})\vec{e}_{ij} + B_{ij}\left(\tilde{\rho}_i + \tilde{\rho}_j\right)\omega^d(r_{ij})\vec{e}_{ij}, \tag{2}$$

$$\vec{f}_{ij}^{\,D} = -\gamma_{ij}\omega^D(r_{ij})\left(\vec{e}_{ij}\cdot\vec{v}_{ij}\right)\vec{e}_{ij}, \tag{3}$$

$$\vec{f}_{ij}^{\,R} = \sigma_{ij}\omega^R(r_{ij})\zeta_{ij}\Delta t^{-1/2}\vec{e}_{ij}, \tag{4}$$

where A_{ij} and B_{ij} are the amplitudes of the attractive and repulsive forces, respectively. To obtain the temperature-dependent properties, the two parameters are modeled as a function of temperature in this work. $\omega^C(r_{ij}) = (1 - r_{ij}/r_C)$ and $\omega^d(r_{ij}) = (1 - r_{ij}/r_d)$ represent the distance-dependent weight functions, which vanish if the distance is larger than the corresponding cutoff radii, r_C and r_d, respectively. $\tilde{\rho}_i$ and $\tilde{\rho}_j$ are the weighted local density functions of particles i and j, respectively, which are given by $\tilde{\rho}_i = \sum_{j\neq i}\omega^\rho(r_{ij})$, where the weight function of the local density $\omega^\rho(r_{ij}) = 105/16\pi r_d^3 \cdot (1 + 3r_{ij}/r_d)(1 - r_{ij}/r_d)^3$. Here, $\int_0^\infty d^3\mathbf{r}\omega^\rho(r_{ij}) = 1$ since the weight function is normalized by the factor $105/16\pi r_d^3$. $\zeta_{ij} = \zeta_{ji}$ is a random number with zero mean and a variance of unity, which conserves the momentum of the interacting

pair of particles. The dissipative coefficient γ_{ij} and random coefficient σ_{ij} satisfy the fluctuation–dissipation theorem, which requires

$$\sigma_{ij}^2 = \frac{4\gamma_{ij}k_B T_i T_j}{(T_i + T_j)}, \quad \omega^R(r_{ij}) = \left[\omega^D(r_{ij})\right]^{1/2}, \tag{5}$$

where k_B and T are the Boltzmann's constant and the system equilibrium temperature, respectively. $\omega^D(r_{ij})$ and $\omega^R(r_{ij})$ are the weight functions for the dissipative and random forces, respectively, where $\omega^D(r_{ij}) = (1 - r_{ij}/r_C)^{s_v}$ for $r_{ij} < r_C$. s_v depends on the viscosity of the fluid. Here, we adopt the modified expression proposed by Li *et al.*[36] to obtain the temperature-dependent viscosity.

As mDPDe satisfies energy conservation, the heat transfer between particles is realized by the exchange of internal energy, which is an additional property and expressed as[23]

$$C_v \frac{dT_i}{dt} = \sum_{j \neq i} \left(q_{ij}^{V_h} + q_{ij}^{C_h} + q_{ij}^{R_h} \right), \tag{6}$$

where the heat flux q_i is the sum of the heat flux due to collisions q_{ij}^C, viscous heating due to mechanical energy q_{ij}^V, and heat flow due to thermal fluctuations q_{ij}^R within the truncation radius. C_V is the heat capacity at constant volume, which is normalized by k_B. The specific expressions are given by

$$q_{ij}^{V_h} = \frac{1}{2C_v}\left[\omega^D(r_{ij})\left\{\gamma_{ij}\left(\vec{e}_{ij}\cdot\vec{v}_{ij}\right)^2 - \frac{\sigma_{ij}^2}{m_i}\right\} - \sigma_{ij}\omega^R(r_{ij})\left(\vec{e}_{ij}\cdot\vec{v}_{ij}\right)\zeta_{ij}\right], \tag{7}$$

$$q_{ij}^{C_h} = \kappa_{ij}\omega^{CT}(r_{ij})\left(\frac{1}{T_i} - \frac{1}{T_j}\right), \tag{8}$$

$$q_{ij}^{R_h} = \alpha_{ij}\omega^{RT}(r_{ij})\zeta_{ij}^e \Delta t^{-1/2}, \tag{9}$$

where k_{ij} and α_{ij} represent the strengths of the conductive and random heat fluxes, respectively. They are given by

$$\kappa_{ij} = k_o k_B T_{eq}^2 \left(\frac{\varepsilon_i + \varepsilon_j}{2k_B T_{eq}}\right)^{n_k}, \tag{10}$$

$$\alpha_{ij} = \sqrt{2k_B\kappa_{ij}}, \tag{11}$$

where ϵ_i is the internal energy. k_o is a positive constant that determines the thermal conductivity of mDPDe particles. T_{eq} is the equilibrium temperature of the system and n_κ is a constant that was chosen to be 2 in the previous work.[24,28] κ is a constant related to the thermal conductivity of mDPDe particles. $\omega^{CT}(r_{ij})$ and $\omega^{RT}(r_{ij})$ are the weight functions, which are related as follows: $\omega^{CT}(r_{ij}) = [\omega^{RT}(r_{ij})]^2$ and $\omega^{CT}(r_{ij}) = (1 - r_{ij}/r_{CT})^{s_T}$. s_T was set to 2 in a previous paper.[36] In this work, to capture the Prandtl number of the system correctly, we fit an equation that depends on temperature. $\zeta_{ij}^e = -\zeta_{ji}^e$ is a random number with properties similar to those of ζ_{ij}, which also conserves the energy of the interacting pair of particles.[23]

III. RESULTS AND DISCUSSION

We develop an alternative model for simulating thermocapillary droplet motion on solid surfaces by combining many-body dissipative particle dynamics and energy-conservative dissipative particle dynamics. Based on the governing equations, we clarify the effective temperature-dependent coefficients setup, which is important for capturing the correct properties of different kinds of liquid systems including density, surface tension, and viscosity. And then, the main dimensionless numbers which are related with the diffusion properties are checked. At the end, a classical case of the thermocapillary droplet motion is adopted to validate our proposed model.

A. Temperature-dependent properties

To validate the hydrodynamic properties of the proposed non-isothermal mDPDe model, we simulated the periodic Poiseuille flow of a simple mDPDe fluid and compared the results with those from an isothermal mDPD model. Two equal forces in opposite directions ($F = 0.02$) were applied on each mDPDe particle to drive the flow. The mDPDe parameters for the periodic Poiseuille flow are listed in the caption of Fig. 1. The computational domain was divided into 50 bins along the z-direction. The equilibrium velocity profiles are shown in Fig. 1, which were obtained by averaging a sufficient number of samples. The results agree with those of the mDPD model, illustrating that we can use the modified mDPDe model to obtain the same hydrodynamic properties as mDPD.

The next test case for validation is heat conduction between a cold wall and a hot wall. A schematic of the geometry is shown in Fig. 2. The stationary fluid is confined between the hot wall at $T_H = 1.2$ and the cold wall at $T_C = 1.0$. We ran tests with different values of the coefficients: constant attractive coefficient $A = -40$ and constant repulsive coefficient $B = 25$, constant $A = -40$ and temperature-dependent $B = 25k_BT$, and temperature-dependent $A = -40k_BT$ and constant $B = 25$. Figure 3(a) shows that the temperature profile of the fluid in the tests has a linear spatial distribution for steady-state heat conduction, which obeys Fourier's law. However, as shown in Fig. 3(b), the density in these systems changed in different ways with an increase in temperature. For real water, the density decreases with increasing temperature in most of the range from 273 to 373 K. Thus, using a temperature-dependent repulsive parameter $B = 25k_BT$ and a constant value for the attractive parameter $A = -40$ is better for simulating the heat conduction between liquid water and the substrate.

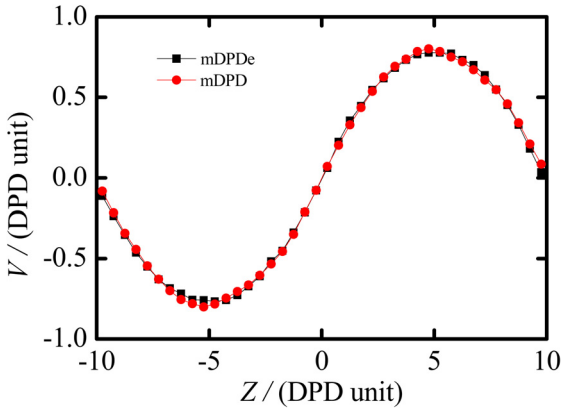

FIG. 1. Velocity profile for the periodic Poiseuille flow along the z-direction with attractive coefficient $A = -40$, repulsive coefficient $B = 25$, temperature $k_BT = 1.0$, dissipative coefficient $\gamma = 8.0$, and external force $F = 0.02$.

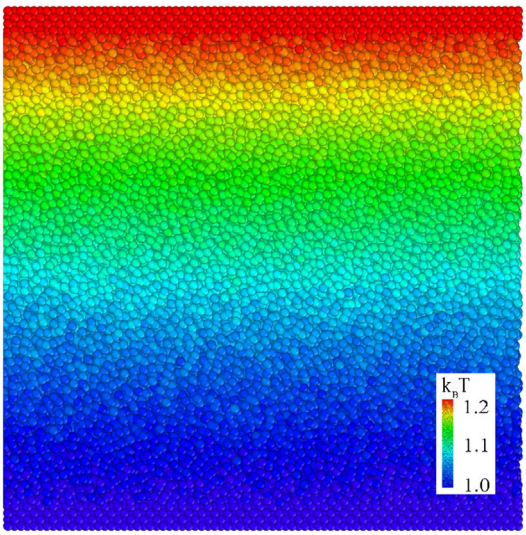

FIG. 2. Schematic of the geometry for steady-state heat conduction between a cold wall T_C (blue) and a hot wall T_H (red).

The above two cases validated the modified mDPDe model. For an isothermal fluid system, the proposed model correctly captures the behavior of the fluid, as mDPD does. For a non-isothermal fluid system, the proposed model can reproduce Fourier's law for heat conduction between a hot wall and a cold wall. A bounce-back boundary condition is adopted in this model although other boundary conditions have been developed for DPD models, such as arbitrary boundary conditions,[46] and a modified version for complex geometry.[47] Our next objective is to construct a model to capture the dynamic properties of common fluids in non-isothermal systems.

Liquid water was used as an example fluid in the present study. We determine the self-diffusivity, kinematic viscosity, surface tension, density, and thermal diffusivity at various temperatures. Thus, these are output properties instead of input parameters. Their exact values can be obtained by simulating an mDPDe system.

The compressibility of a liquid system is $\kappa_c^{-1} = (\partial p/\partial \rho)_T/k_BT$. The pressure of the mDPD fluid system can be approximated as

$$p = \rho k_B T + \alpha A \rho^2 + 2\alpha B r_d^4 \left(\rho^3 - c\rho^2 + d\right),$$

where $\alpha = 0.101 \pm 0.001$, $c = 4.16 \pm 0.02$, and $d = 18 \pm 1$.[14] The compressibility of the fluid system can be derived as

$$\kappa_c^{-1} = 1 + 1/k_BT\left[2\alpha A\rho + 2\alpha B r_d^4\left(3\rho^2 - 2c\right)\right].$$

Thus, a dimensionless coefficient corresponding to the compressibility of the liquid system is $\kappa_c^{-1} = [L]^3/\rho k_B T \beta_T$.[13] For liquid water at 300 K, the thermal term is $k_BT = 4.142 \times 10^{-21}$ kg m^2 s^{-2} and $\beta_T = 4.503 \times 10^{-10}$ m s^2/kg. For an mDPDe system with density $\rho = 6.8$, $A = -40$, and $B = 25$, the corresponding scaling length is $[L] \approx 1.18$ nm. The dimensionless coefficient was approximated as 130, which is larger than that from the pressure (76.3). Thus, the compressibility of the fluid system could be underestimated, as we adopt $A = -40$ and $B = 25k_BT$ to determine the basic properties, including density ρ, surface tension σ, and kinematic viscosity ν. We scale these parameters by the values for water at different temperatures. The underestimation is acceptable, as the error from the density and pressure measurement could be magnified by the coefficients in the relation between the compressibility and the parameters of the mDPDe system.

We can determine the self-diffusivity of the mDPDe system from the mean square displacement (MSD)

$$D = \lim_{t\to\infty} \frac{1}{6t} \langle |\mathbf{r}(t) - \mathbf{r}(0)|^2 \rangle, \tag{12}$$

where $|\mathbf{r}(t) - \mathbf{r}(0)|^2$ is the mean square displacement (MSD). Figure 4 shows the MSD of the system from $k_BT = 1.0$ to 1.25. The MSD has been scaled by 6.0. Thus, the slope of the line is the self-diffusivity for each case. This figure shows that the diffusivity increased as the temperature increased.

The temperature unit was characterized as $T_R = 300$ K. The mass, time, and length units were characterized as[19,48] $M_{DPD} = L_{DPD}^3 d^*/d$, $T_{DPD} = (M_{DPD}\sigma/\sigma^*)^{1/2}$, and $L_{DPD}^2/T_{DPD} = \nu^*/\nu$. The basic properties of water are the density ρ, surface tension σ, and viscosity ν, while the corresponding parameters in an mDPDe system are

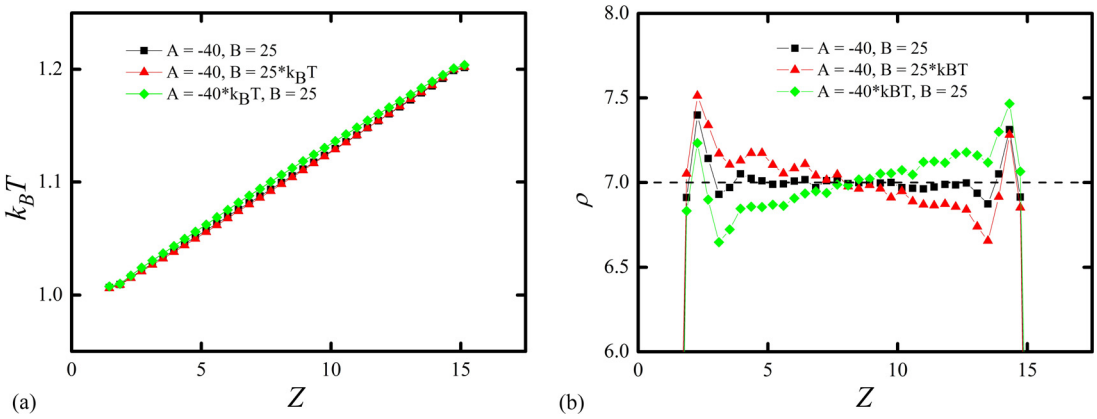

FIG. 3. Temperature (a) and density (b) profiles for heat conduction between a hot wall ($T_H = 1.2$) and a cold wall ($T_C = 1.0$) with different values of the conservative parameters A and B. All the simulations used 18 500 mDPDe particles in a computational domain $40.0 \times 4.0 \times 17.0$ in mDPDe units.

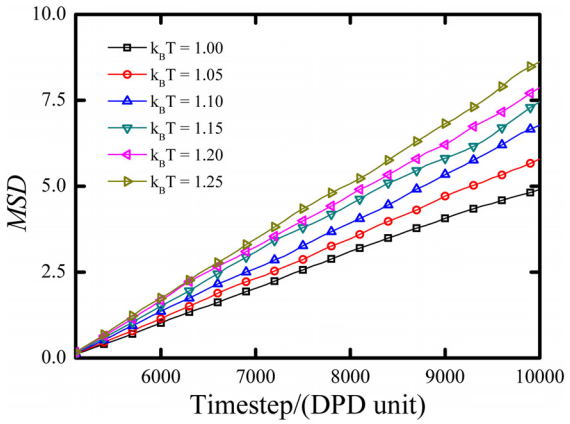

FIG. 4. Mean-square displacement (scaled by 6.0) of mDPDe particles for different temperatures. The slopes of the lines are the self-diffusivity of mDPDe fluid.

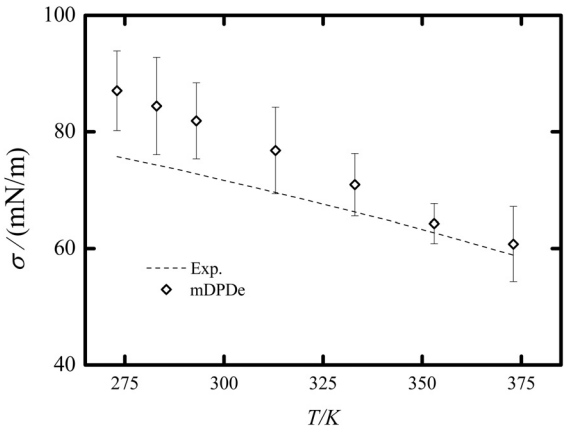

FIG. 5. Comparison of experimental data and the results of mDPDe simulations for the temperature-dependent surface tension σ for temperatures from 273 to 373 K.

marked with an asterisk. For each group of these properties, we can obtain the corresponding length $[\mathrm{L}](T_i)$, mass $[\mathrm{M}](T_i)$, and time $[\mathrm{T}](T_i)$ units according to the system of equations mentioned above. Based on the test results shown in Table I, a series of these basic units can be obtained. Since all the length units $[\mathrm{L}](T_i)$ fluctuate within one order of magnitude around 10^{-9} m, we adopt the average value of the series results derived from the table to describe the length unit of the system for temperatures from 273 to 373 K as well as the time and mass units. Thus, the length, time, and mass units of the system were, respectively, $[\bar{L}] = 1.18 \times 10^{-9}$ m, $[\bar{T}] = 5.58 \times 10^{-12}$ s, and $[\bar{M}] = 2.73 \times 10^{-25}$ kg.

The kinematic viscosity of the mDPDe system is computed for a periodic Poiseuille flow. The velocity profiles obtained for the periodic Poiseuille are shown in Fig. 1. The kinematic viscosity can be determined by fitting the velocity profile with the analytical solution $u(z) = g_x z(d - |z|)/2\nu$, where ν is the kinematic viscosity, $g_x = 0.02$ is the body force applied to the mDPDe particles, and $d = 10.0$ is the half-length of the computational domain in the z-direction.

Using this scaling, we obtaine the surface tension from the mDPDe simulations, as shown in Fig. 5. It agrees well with the experimental data, in which the error bars are from ten times simulations with the same parameters. Moreover, the simulations show that the corresponding Schmidt number is also in good agreement with that of real water, as shown in Fig. 6(a). Overall, the proposed mDPDe model correctly reproduces the temperature-dependent dynamic properties, including the diffusivity, kinematic viscosity, and Schmidt number. The values are comparable to the experimental data for liquid water for temperatures from 273 to 373 K. The relative errors of the Schmidt number are generally less than 10%.

For the thermal conductivity in the liquid system, we adopte the *heat conduction analog* of periodic Poiseuille flow, which was proposed by Li *et al.*,[36] to obtain the thermal diffusivity of an mDPDe fluid. A schematic of the geometry and the temperature profile is shown in Figs. 7 and 8, respectively.

The result can be characterized by the Prandtl number $Pr = \nu/\lambda$, which is the ratio of the momentum diffusivity ν to the thermal diffusivity λ. Figure 6(b) compares the temperature-dependent Prandtl number of liquid water from the mDPDe simulations with experimental data. The error or difference between the numerical results and the experimental data varied for different values of the parameter s_T. In particular, for $s_T = 2.0$, which was the default value, the error at high temperatures is larger than 15%. For $s_T = 1.0$, the Prandtl number at low temperatures is lower than the experimental value by over 18%. Using the series of values of s_T at various temperatures, we obtaine an empirical formula to accurately describe the Prandtl number in the mDPDe model: $s_T = -0.75k_BT + 1.78$. The values of the Prandtl number obtained for an mDPDe fluid with this formula are consistent with the experimental data. The relative error is less than 10% for the entire temperature range from 273 to 373 K.

TABLE I. Basic properties from the mDPDe model at various temperatures.

T_i (K)	k_BT	σ	N	P
273	0.91	9.93	7.71	7.00
283	0.943 35	9.63	5.49	6.92
293	0.976 67	9.34	4.04	6.81
313	1.043 3	8.76	2.91	6.62
333	1.11	8.09	1.89	6.43
353	1.176 67	7.33	1.41	6.25
373	1.243 3	6.93	1.01	6.08

B. Thermocapillary motion of a droplet

Based on the modified mDPDe, we investigate the thermocapillary motion of a droplet on a hydrophobic substrate with a temperature gradient, as shown in Fig. 9. This phenomenon has been investigated by other theoretical, experimental, and numerical methods,[49,50] which suggested that the velocity depends on the temperature difference between the ends of the droplet due to the temperature gradient. For the interactions between liquid particles due to the conservative force, $A = -40$ and $B = 25k_BT$. For the interactions between solid and liquid particles, $A_{sl} = -15$ and $B_{sl} = 12.5$, for which the static contact angle was around 120°. The effect of the roughness of

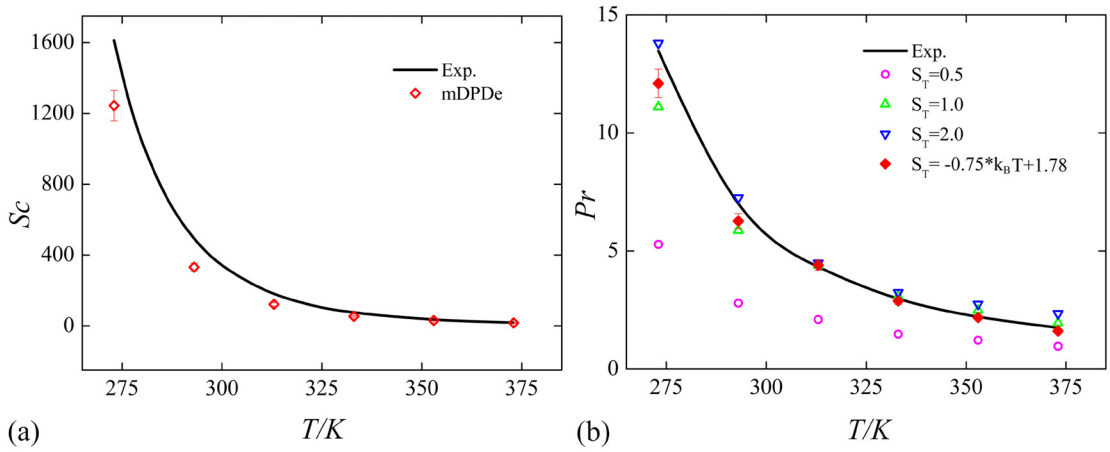

FIG. 6. Comparison of experimental data and the results of mDPDe simulations for the temperature-dependent (a) Schmidt number and (b) Prandtl number of liquid water for temperatures from 273 to 373 K.

the surface on the sliding motion of the droplet is neglected in this work.[51]

In the simulations, we first set a droplet on a hydrophobic substrate with a constant temperature $k_BT = 1.0$. After the droplet has entered an equilibrium state on the substrate, i.e., it has formed a spherical cap (around 10 000 time steps), a temperature gradient is applied to the substrate. The droplet then spontaneously moves from the hot to the cold area along the substrate due to the Marangoni effect (around 90 000 time steps). Since the time step is 0.005, the total time for the Marangoni effect is around 450 in mDPDe units.

We test three different cases with various sizes of droplets on the same substrate. Based on the scaling mentioned above, the sizes of the water droplets in the simulations are as follows: (1) 8.3 nm (8061 mDPDe particles), (2) 9.5 nm (14 000 mDPDe particles), and (3) 11 nm (22 408 mDPDe particles). The length of the substrate is around 70 nm along the x-direction, 45 nm along the y-direction, and 1.2 nm along the z-direction. It has 14 400 mDPDe particles. The temperature of the substrate varies from 360 to 300 K along the x-direction. The temperature gradient is around 0.857 K/nm. A bounce-back boundary condition is used in this model, as has been used in the previous work.[52]

We measure how far the droplet moved due to the Marangoni effect and then calculate the velocity of the droplets, which increased as the temperature gradient increased. The Marangoni effect can be affected by the random numbers used in the mDPDe simulations, which was also observed in the previous work.[19] The comparison of the results from the mDPDe simulation, the theoretical analysis, and the DVDWT method[50] in Fig. 10 suggests that this modified mDPDe model can effectively capture the thermocapillary motion of nanodroplets on hydrophobic substrates with a temperature gradient.

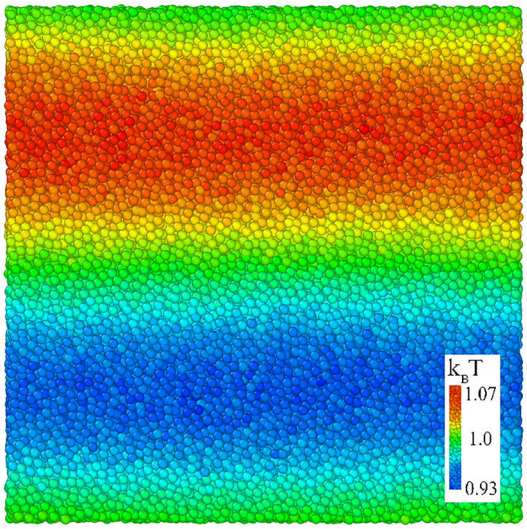

FIG. 7. Schematic of *heat conduction analog* of periodic Poiseuille flow.[36] In this system, a heat source is applied in the upper half domain, while a sink source with same amplitude is applied in the lower half domain. When the system reaches an equilibrium state, the temperature profile will be like the velocity distribution in the Poseuille flow which is shown in Fig. 1.

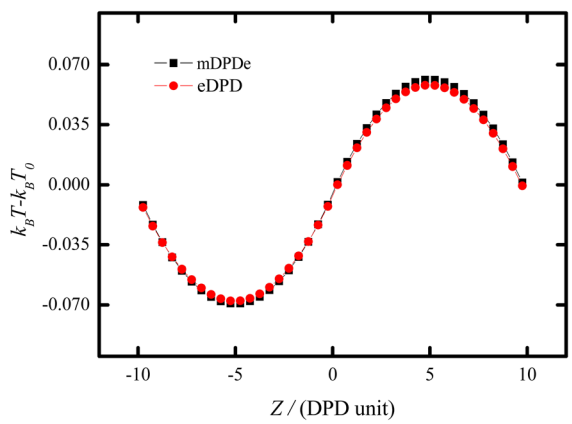

FIG. 8. Comparison of the temperature profiles obtained from mDPDe and eDPD simulations using the *heat conduction analog* of periodic Poiseuille flow for different temperatures.

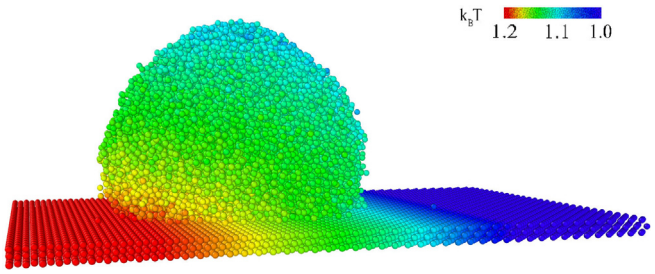

FIG. 9. Schematic of droplet motion induced by a thermal gradient on a hydrophobic substrate. The temperature of the hot end (red) was $T = 360$ K, and the cold end (blue) $T = 300$ K. The length of the substrate was around 70 nm, and it had a temperature gradient of 0.857 K/nm.

In the comparison, the velocity $V = 400$ m/s and the temperature of the water $T = 600$ K. These values are used to scale the results.[50]

IV. CONCLUSIONS

The proposed mDPDe model can correctly determine the temperature-dependent properties, including density, surface tension, and Schmidt and Prandtl numbers. It can be adopted to investigate the motion of a droplet on a substrate induced by the Marangoni effect. The relations between liquid–vapor surface tension of an mDPDe fluid and the parameters in the conservative force are analyzed. By including the dissipative and random forces using weighting terms, the temperature-dependent self-diffusivity and thermal diffusivity are obtained. The liquid–vapor surface tension, viscosity, momentum, and thermal diffusivity of liquid water at various temperatures from 273 to 373 K are used as a benchmark to verify the model. The results show that the proposed model can correctly reproduce the temperature-dependent properties, including the liquid–vapor surface tension, Schmidt number, and Prandtl number. The values are consistent with the experimental data available for liquid water. Moreover, an empirical formula for obtaining a more accurate Prandtl number at high temperatures is obtained from the mDPDe simulations.

The modified mDPDe model is used to simulate the thermocapillary motion of a droplet on a hydrophobic substrate with a temperature gradient. The results show that the velocity of a droplet increased as the temperature difference between the advancing and receding triple-phase contact area increased. The results are in good agreement with a theoretical analysis and DVDWT simulations.[50] Although we test this model for liquid water between 273 and 373 K, the method proposed in the present work for modeling temperature-dependent properties is not limited to water and could readily be extended to other fluids and phenomena.[53–56]

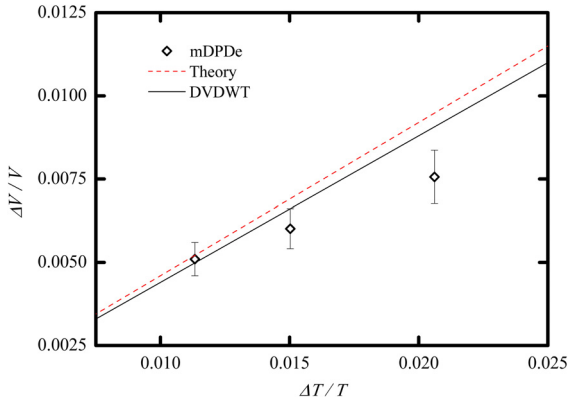

FIG. 10. Comparison of the results from the mDPDe simulation, the theoretical analysis, and the DVDWT method.[50] Velocity $V = 400$ m/s and temperature $T = 600$ K, as described in Ref. 50.

ACKNOWLEDGMENTS

This work was supported by the National Natural Science Foundation of China (Grant Nos. 11921002, 12032014, 11872227, 12172189, 11872283, 12102218, 12002242, and 12002212), the China Postdoctoral Science Foundation (Nos. 2020M680525 and 2021M701905), and the Shanghai Science and Technology Talent Program (No. 20YF1432800).

AUTHOR DECLARATIONS

Conflict of Interest

The authors have no conflicts to disclose.

Author Contributions

Kaixuan Zhang, Jie Li, and Wei Fang contributed to this work equally.

DATA AVAILABILITY

The data that support the findings of this study are available within the article.

REFERENCES

[1]P. Hoogerbrugge and J. Koelman, "Simulating microscopic hydrodynamic phenomena with dissipative particle dynamics," Europhys. Lett. **19**, 155–160 (1992).
[2]S. Chen, N. Phan-Thien, B. C. Khoo, and X. J. Fan, "Flow around spheres by dissipative particle dynamics," Phys. Fluids **18**, 103605 (2006).
[3]X. Li, J. Guo, Y. Liu, and H. Liang, "Microphase separation of diblock copolymer poly(styrene-b-isoprene): A dissipative particle dynamics simulation study," J. Chem. Phys. **130**, 074908 (2009).
[4]T. Ye, D. Pan, C. Huang, and M. Liu, "Smoothed particle hydrodynamics (SPH) for complex fluid flows: Recent developments in methodology and applications," Phys. Fluids **31**, 011301 (2019).
[5]X. J. Fan, N. Phan-Thien, S. Chen, X. H. Wu, and T. Y. Ng, "Simulating flow of DNA suspension using dissipative particle dynamics," Phys. Fluids **18**, 063102 (2006).
[6]T. Ye, N. Phan-Thien, B. C. Khoo, and C. T. Lim, "Dissipative particle dynamics simulations of deformation and aggregation of healthy and diseased red blood cells in a tube flow," Phys. Fluids **26**, 111902 (2014).
[7]T. Ye, N. Phan-Thien, B. Cheong Khoo, and C. Teck Lim, "Numerical modelling of a healthy/malaria-infected erythrocyte in shear flow using dissipative particle dynamics method," J. Appl. Phys. **115**, 224701 (2014).
[8]G. Li, T. Ye, S. Wang, X. Li, and R. UI Haq, "Numerical design of a highly efficient microfluidic chip for blood plasma separation," Phys. Fluids **32**, 031903 (2020).
[9]X. Qi, S. Wang, S. Ma, K. Han, and X. Li, "Quantitative prediction of flow dynamics and mechanical retention of surface-altered red blood cells through a splenic slit," Phys. Fluids **33**, 051902 (2021).
[10]X. Qi, S. Wang, S. Ma, K. Han, X. Bian, and X. Li, "Quantitative prediction of rolling dynamics of leukocyte-inspired microroller in blood flow," Phys. Fluids **33**, 121908 (2021).

[11]C. Wu, S. Wang, X. Qi, W. Yan, and X. Li, "Quantitative prediction of elongation deformation and shape relaxation of a red blood cell under tensile and shear stresses," Phys. Fluids **33**, 111906 (2021).
[12]Z. Xu, P. Meakin, A. Tartakovsky, and T. D. Scheibe, "Dissipative-particle-dynamics model of biofilm growth," Phys. Rev. E **83**, 066702 (2011).
[13]R. Groot and P. Warren, "Dissipative particle dynamics: Bridging the gap between atomistic and mesoscopic simulation," J. Chem. Phys. **107**, 4423–4435 (1997).
[14]P. B. Warren, "Vapor-liquid coexistence in many-body dissipative particle dynamics," Phys. Rev. E **68**, 066702 (2003).
[15]Z. Li, G.-H. Hu, Z.-L. Wang, Y.-B. Ma, and Z.-W. Zhou, "Three dimensional flow structures in a moving droplet on substrate: A dissipative particle dynamics study," Phys. Fluids **25**, 072103 (2013).
[16]Y. X. Wang and S. Chen, "Numerical study on droplet sliding across micropillars," Langmuir **31**, 4673–4677 (2015).
[17]K. Zhang, Z. Li, and S. Chen, "Analytical prediction of electrowetting-induced jumping motion for droplets on hydrophobic substrates," Phys. Fluids **31**, 081703 (2019).
[18]C. Lin, D. Cao, D. Zhao, P. Wei, S. Chen, and Y. Liu, "Dynamics of droplet impact on a ring surface," Phys. Fluids **34**, 012004 (2022).
[19]M. Arienti, W. Pan, X. Li, and G. Karniadakis, "Many-body dissipative particle dynamics simulation of liquid/vapor and liquid/solid interactions," J. Chem. Phys. **134**, 204114 (2011).
[20]D. Pan, G. Zhao, Y. Lin, and X. Shao, "Mesoscopic modelling of microbubble in liquid with finite density ratio of gas to liquid," Europhys. Lett. **122**, 20003 (2018).
[21]C. J. Mo, L. Z. Qin, and L. J. Yang, "Hypernetted-chain-like closure of Ornstein–Zernike equation in multibody dissipative particle dynamics," Phys. Rev. E **96**, 043303 (2017).
[22]C. Zhao, J. Zhao, T. Si, and S. Chen, "Influence of thermal fluctuations on nanoscale free-surface flows: A many-body dissipative particle dynamics study," Phys. Fluids **33**, 112004 (2021).
[23]P. Español, "Dissipative particle dynamics with energy conservation," Europhys. Lett. **40**, 631–636 (1997).
[24]R. Qiao and P. He, "Simulation of heat conduction in nanocomposite using energy-conserving dissipative particle dynamics," Mol. Simul. **33**, 677–683 (2007).
[25]A. Chaudhri and J. Lukes, "Multicomponent energy conserving dissipative particle dynamics: A general framework for mesoscopic heat transfer applications," J. Heat Transfer **131**, 033108 (2009).
[26]Z.-H. Cao, K. Luo, H.-L. Yi, and H.-P. Tan, "Energy conservative dissipative particle dynamics simulation of mixed convection in eccentric annulus," Int. J. Heat Mass Transfer **74**, 60–76 (2014).
[27]Y.-X. Zhang, X.-P. Luo, H.-L. Yi, and H.-P. Tan, "Energy conserving dissipative particle dynamics study of phonon heat transport in thin films," Int. J. Heat Mass Transfer **97**, 279–288 (2016).
[28]E. Abu-Nada, "Natural convection heat transfer simulation using energy conservative dissipative particle dynamics," Phys. Rev. E **81**, 056704 (2010).
[29]E. Abu-Nada, "Energy conservative dissipative particle dynamics simulation of natural convection in liquids," J. Heat Transfer **133**, 112502 (2011).
[30]E. Abu-Nada, "Dissipative particle dynamics simulation of combined convection in a vertical lid driven cavity with a corner heater," Int. J. Therm. Sci. **92**, 72–84 (2015).
[31]E. Abu-Nada, "Assessment of dissipative particle dynamics to simulate combined convection heat transfer: Effect of compressibility," Int. Commun. Heat Mass Transfer **61**, 49–60 (2015).
[32]E. Abu-Nada, "Dissipative particle dynamics simulation of natural convection using variable thermal properties," Int. Commun. Heat Mass Transfer **69**, 84–93 (2015).
[33]E. O. Johansson, T. Yamada, B. Sunden, and J. Yuan, "Modeling mesoscopic solidification using dissipative particle dynamics," Int. J. Therm. Sci. **101**, 207–216 (2016).
[34]M. Ripoll, P. Espaol, and M. H. Ernst, "Dissipative particle dynamics with energy conservation: Heat conduction," Int. J. Mod. Phys. C **9**, 1329–1338 (1998).
[35]P. He and R. Qiao, "Self-consistent fluctuating hydrodynamics simulations of thermal transport in nanoparticle suspensions," J. Appl. Phys. **103**, 783–788 (2008).
[36]Z. Li, Y.-H. Tang, H. Lei, B. Caswell, and G. E. Karniadakis, "Energy-conserving dissipative particle dynamics with temperature-dependent properties," J. Comput. Phys. **265**, 113–127 (2014).
[37]T. Yamada, E. O. Johansson, J. Yuan, and B. Sunden, "Dissipative particle dynamics simulations of water droplet flows in a submicron parallel-plate channel for different temperature and surface-wetting conditions," Numer. Heat Transfer, Part A **70**, 1–18 (2016).
[38]L. Wang, J. Dai, P. Hao, F. He, and X. Zhang, "Mesoscopic dynamical model of ice crystal nucleation leading to droplet freezing," ACS Omega **5**, 3322–3332 (2020).
[39]C. Wang, X. Wu, P. Hao, F. He, and X. Zhang, "Study on a mesoscopic model of droplets freezing considering the recalescence process," Phys. Fluids **33**, 092001 (2021).
[40]J. Fan, H. Wu, and F. Wang, "Evaporation-driven liquid flow through nanochannels," Phys. Fluids **32**, 012001 (2020).
[41]W. Zhao, H. Ma, W. Ji, W. Li, J. Wang, Q. Yuan, Y. Wang, and D. Lan, "Marangoni-driven instability patterns of an *N*-hexadecane drop triggered by assistant solvent," Phys. Fluids **33**, 024104 (2021).
[42]S. Kumar, "Insight on the evaporation dynamics in reducing the COVID-19 infection triggered by respiratory droplets," Phys. Fluids **33**, 072004 (2021).
[43]Z. W. Jiang, R. Chen, T. Wu, H. Ding, and E. Q. Li, "Contactless transport of sessile droplets," Phys. Fluids **33**, 112115 (2021).
[44]J.-Y. Chen, P. Gao, Y.-T. Xia, E.-Q. Li, H.-R. Liu, and H. Ding, "Early stage of delayed coalescence of soluble paired droplets: A numerical study," Phys. Fluids **33**, 092005 (2021).
[45]J. B. Avalos and A. D. Mackie, "Dissipative particle dynamics with energy conservation," Europhys. Lett. **40**, 141–146 (1997).
[46]Z. Li, X. Bian, Y. H. Tang, and G. E. Karniadakis, "A dissipative particle dynamics method for arbitrarily complex geometries," J. Comput. Phys. **355**, 534–547 (2018).
[47]C. Lin, S. Chen, and L.-L. Xiao, "New dissipative particle dynamics boundary condition for complex geometry," Acta Phys. Sin. **68**, 140204 (2019).
[48]K. Zhang, Z. Li, M. Maxey, S. Chen, and G. E. Karniadakis, "Self-cleaning of hydrophobic rough surfaces by coalescence-induced wetting transition," Langmuir **35**, 2431–2442 (2019).
[49]F. Brochard, "Motions of droplets on solid surfaces induced by chemical or thermal gradients," Langmuir **5**, 432–438 (1989).
[50]X. Xu and T. Qian, "Thermal singularity and droplet motion in one-component fluids on solid substrates with thermal gradients," Phys. Rev. E **85**, 061603 (2012).
[51]C. Lv, C. Yang, P. Hao, F. He, and Q. Zheng, "Sliding of water droplets on microstructured hydrophobic surfaces," Langmuir **26**, 8704–8708 (2010).
[52]Y. Wang, J. Zhao, D. Zhang, M. Jian, and X. Zhang, "Droplet sliding: The numerical observation of multiple contact angle hysteresis," Langmuir **35**, 9970–9978 (2019).
[53]Q. Rao, Y. Xia, J. Li, J. McConnell, J. Sutherland, and Z. Li, "A modified many-body dissipative particle dynamics model for mesoscopic fluid simulation: Methodology, calibration, and application for hydrocarbon and water," Mol. Simul. **47**, 363–375 (2021).
[54]Q. Rao, Y. Xia, J. Li, M. Deo, and Z. Li, "Flow reduction of hydrocarbon liquid in silica nanochannel: Insight from many-body dissipative particle dynamics simulations," J. Mol. Liq. **344**, 117673 (2021).
[55]Y. Cheng, E. Li, J. Wang, P. Yu, and Y. Sui, "Rapid droplet spreading on a hot substrate," Phys. Fluids **33**, 092103 (2021).
[56]M. Frank, M. Lappa, and P. Capobianchi, "Investigation of thermocapillary migration of nanodroplets using molecular dynamics," Phys. Fluids **33**, 042110 (2021).